Journal of Physics and Its Applications

Journal homepage : https://ejournal2.undip.ac.id/index.php/jpa/index

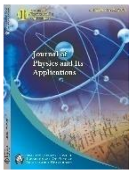

Antibacterial Activity of Green-Synthesized Silver Nanoparticles from Black Betel Leaf Extract and Polyvinyl Alcohol

Iftitahul Khoiriyah[1], Jezzy Puspa Ayu Wardani[1], Dimas Rahadian Aji Muhammad[2], and Lita Rahmasari[1]*

[1]Department of Physics Education, Faculty of Teacher Training and Education, Universitas Sebelas Maret, Surakarta, Indonesia
[2]Department of Food Science and Technology, Faculty of Agriculture, Universitas Sebelas Maret, Surakarta, Indonesia

**Corresponding author:* lita@staff.uns.ac.id

A R T I C L E I N F O

Article history:
Received: 16 May 2026
Accepted: 03 August 2026
Available online: 31 August 2026

Keywords:
Silver nanoparticles
Green synthesis
Black betel leaf
Polyvinyl alcohol
Antibacterial

A B S T R A C T

Black betel leaf extract contains reducing agents like flavonoids, which can reduce the size of silver particles to nanoscale. Meanwhile, Polyvinyl alcohol (PVA) is used to prevent the agglomeration of silver nanoparticles (AgNPs). This study aimed to determine the antibacterial activity of AgNPs synthesized from black betel leaf extract and PVA against *Staphylococcus aureus* and *Escherichia coli* bacteria. PVA was varied at concentrations of 0.5 g, 1 g, and 1.5 g in 25 mL of deionized water, which was then mixed with 25 mL of black betel leaf extract. AgNPs were produced through a green synthesis process using the sol-gel technique, involving extraction, synthesis, characterization, and data analysis. The resulting AgNPs were stable across variations in polymer mass, with maximum wavelength absorption ranging from 403 nm to 440 nm. Analysis showed that the AgNPs possessed a Face Centered Cubic (FCC) crystal structure with particle sizes between 12.4 nm and 14.7 nm. Furthermore, the AgNPs were surrounded by various organic molecules such as terpenoids, alcohols, ketones, aldehydes, and carboxylic acids. The most potent antibacterial nanoparticles were the AgNPs synthesized with 0.5 grams of PVA. These AgNPs demonstrated an inhibition zone of 13.9 mm against *Escherichia coli* and 11.3 mm against *Staphylococcus aureus*.

1. Introduction

Nanotechnology is a rapidly expanding field that has found applications in various sectors, including health, environment, and industry [1]. Nanomaterials are crucial to the advancement of nanotechnology, offering superior properties compared to their bulk counterparts [2]. Based on their dimensionality, NMs can be further divided into four classes. Zero-dimensional nanomaterials (0D) which have nanoscale dimensions with sizes below 100 nm such as nanoparticles, One-dimensional nanomaterials (1D) such as nanotubes, Two-dimensional nanomaterials (2D) such as nanoplates and Three-dimensional nanomaterials (3D) such as nanotubes [3]. Among these, metal nanoparticles have garnered significant research interest due to their unique optical properties that differ from those of macro-sized materials [4].

Silver (Ag) is one of the most frequently used metals in nanoparticle (NP) synthesis due to its low production cost, simple synthesis process, and excellent optical properties [5], [6]. Silver nanoparticles are a promising material for effective antibacterial applications, working through several mechanisms [7]. These include damaging cell membranes, interacting with cell walls, and inhibiting bacterial growth [8]. The effectiveness of silver nanoparticles as an antibacterial agent is attributed to their size and shape. Smaller silver nanoparticles have a larger surface area, which enhances their antibacterial activity [9]. Therefore, it's crucial to study synthesis methods to produce silver nanoparticles with small sizes and a homogeneous size distribution.

Silver nanoparticles are commonly produced using a bottom-up approach [7]. This method is favored because it can create small silver nanoparticles by assembling molecules or atoms and then combining them through a chemical reaction (reduction) [10]. One effective bottom-up technique is biosynthesis, also known as green synthesis. This method is environmentally friendly and reduces hazardous waste [11]. However, a drawback of biosynthesis is its inability to produce silver nanoparticles with a homogeneous size distribution. Therefore, green synthesis methods often need to be combined with other techniques, such as the sol-gel chemical method [12].

The chemical sol-gel technique is a bottom-up approach that yields products with high purity and relatively small particle sizes. Compared with several nanoparticle synthesis methods such as hydrothermal and co-precipitation, the sol-gel method offers better control over particle homogeneity and composition [12,13]. The sol-gel method overcomes green synthesis's shortcomings by yielding homogeneous nanoparticles [12]. Combining the sol-gel method with green synthesis aims to minimize hazardous chemical waste by using bioreductor. This combined approach offers several advantages, including being environmentally friendly, cost-effective, and simple to execute, while also producing homogeneous silver nanoparticles [13].

Bio-reductor are natural reductants derived from natural materials that contain compounds like polysaccharides, flavonoids, and terpenoids [14]. One plant extract with the potential to act as a bio-reductor agent in AgNPs synthesis is black betel leaf extract. This statement is based on the results of the phytochemical test of black betel leaf extract which shows that black betel contains alkaloid, flavonoid, and terpenoid compounds [15]. Flavonoid compounds in black betel leaf extract can function as bioreductors in the synthesis of AgNPs [16]. In addition, AgNPs are prone to aggregation, so a capping agent or stabilizer is needed to prevent aggregation. Polyvinyl alcohol (PVA) is one type of polymer that is effectively used in making AgNPs [17].

Based on this description, the synthesis of silver nanoparticles using black betel leaf extract and PVA needs to be studied further. Studies on using black betel leaf extract as a bio-reducing agent in silver nanoparticle synthesis haven't been conducted before, making this research a novel approach to silver nanoparticle synthesis. In this article, we discuss the biosynthesis of AgNPs using black betel leaf extract and PVA for antibacterial purposes.

2. Methods

2.1. Preparation

$AgNO_3$ 8.49 grams dissolved with 100 mL of aqua bidest and Citric Acid Monohydrate 16.98 grams dissolved with 100 mL of aqua bidest. 1 gram's black betel leaf extract was dissolved with 45 mL of aqua bidest. In addition, polymers in the form of Polyvinyl Alcohol (PVA) as much as 0.5 g (A1), 1 g (A2), and 1.5 g (A3) each were dissolved with 25 mL of aqua bidest [18].

2.2. Fabrication

Green synthesis of silver nanoparticles was carried out by sol-gel method by mixing black betel leaf extract, $AgNO_3$, Citric acid monohydrate, and PVA at 85-90°C for 1.5-2 hours. The formation of silver nanoparticles (AgNPs) through green synthesis was visually confirmed by a change in the solution's color to light brownish color, accompanied by a transformation of the solution's texture into a gel. The solution was put into the oven for 24 hours at 125°C. Then the sample was crushed for 2 hours and washed using a centrifuge for 10 minutes at 6000 rpm. The washed sample was crushed for 2 hours and annealed at 400°C for 2 hours. After the annealing process, the sample was crushed again for 3 hours.

2.3. Characterizations

The synthesized AgNPs were further characterized using several instruments. Initial confirmation of AgNPs presence was performed with a UV-Vis spectrophotometer by examining the wavelength and absorbance of the samples. Subsequently, the morphology, size, and elemental composition of the samples were analyzed using FESEM-EDX. To determine the crystal phase and size, an XRD instrument was utilized. Additionally, FTIR was employed to identify the material's functional groups. Finally, an antibacterial test was conducted using the disc diffusion method against *Staphylococcus aureus* (Gram-positive) and *Escherichia coli* (Gram-negative) to evaluate the antibacterial effectiveness by observing the zone of inhibition.

3. Results and Discussions

3.1. Color change and UV–Vis spectrum analysis

During the synthesis process, the primary indicator for the formation of silver nanoparticles is a visual color change from bright yellow $AgNO_3$ solution to light brownish color [19]–[21]. This color change arises due to the excitation of surface plasmon vibrations with the silver nanoparticles [22]. The transition to a light brownish color signifies the reduction of Ag^+ ions to Ag^0, indicating the successful formation of silver nanoparticles [21]. The synthesis of silver nanoparticles with all PVA variations resulted in a light brownish color solution, which confirms that silver AgNPs were successfully formed.

UV-Vis spectroscopy testing in this study was conducted within the 200-800 nm. The results of the UV-Vis testing are shown in Table 1.

Table 1: The Results of the UV-Vis testing

PVA	Maximum Wavelength (nm)	Absorption (a.u)
A1	404	0.886
A2	403	1.002
A3	440	0.881

The nanoparticle absorption spectrum showed an absorption peak at 403-440 nm, which directly confirms the presence of AgNPs [23]. The SPR band exhibited a red shift from 403 to 440 nm, which can be attributed to an increase in nanoparticle size, as larger AgNPs generally show SPR absorption at longer wavelengths [24]. A similar red shift has been reported previously, where the SPR peak of AgNPs shifted from approximately 420 to 440 nm due to the formation of larger nanoparticles during the reduction of Ag^+ to Ag^0 [25]. According to Car and Krstulović [26], the SPR wavelength is strongly correlated with nanoparticle size; however, variations in SPR position may also arise from differences in particle morphology and the dielectric properties of the surrounding environment. Thus, the red shift observed in the present study can be associated with the growth of AgNPs and remains in agreement with the fundamental SPR characteristics of silver nanoparticles. Based on the UV–Vis spectra, variation A3 exhibited the highest maximum absorption wavelength value (440 nm), indicating the formation of relatively larger AgNPs compared with variations A1 (404 nm) and A2 (403 nm). This red shift suggests an increase in particle size, as larger AgNPs generally exhibit SPR bands at longer wavelengths. In contrast, variations A1 and A2, which showed lower maximum absorption wavelength values, are expected to possess smaller particle sizes. These results provide preliminary information on the size variation of the synthesized AgNPs and can serve as a reference for further characterization.

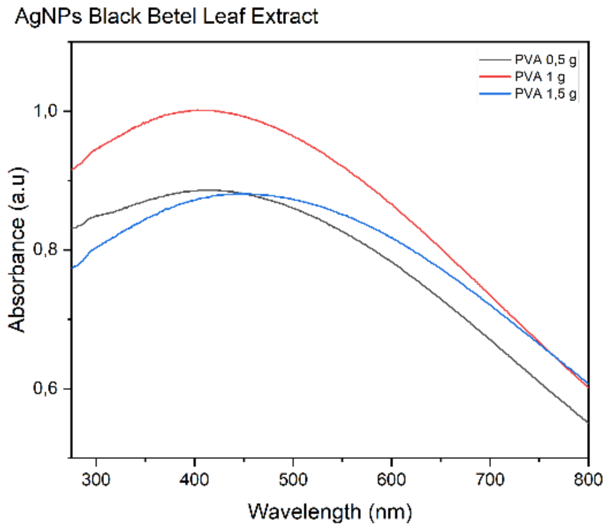

Fig. 1: UV spectrum of AgNPs

Fig. 1 shows UV spectrum of AgNPs prepared by biosynthesis using black betel leaf extract. Based on the graph in Fig. 1, there is a shift in the peak wavelength. A larger peak shift indicates that the stability of silver nanoparticles decreases and is more susceptible to agglomeration or aggregation.

3.2. FESEM-EDX Analysis

Morphological observations were conducted using FESEM at magnifications of 100,000×. The morphological results clearly demonstrate that the AgNPs are spherical, monodisperse, and highly crystalline. Additionally, Fig.2 shows the presence of some larger nanoparticles. This phenomenon indicates that AgNPs tend to undergo agglomeration (aggregation) due to their high energy and surface tension [27]. Agglomeration occurs because of Brownian motion and van der Waals forces within the solution, leading to non-uniform particle size and diameter [28]. The addition of PVA during the synthesis of silver nanoparticles affects the stability of the nanoparticles. Increasing the PVA concentration beyond the optimal level impairs the stability of the silver nanoparticles, leading to agglomeration [29].

The morphological results of variations A1 and A2 show that silver nanoparticles have a spherical structure, with a fairly good distribution although there is a tendency for agglomeration. The A3 variation shows that the particles form agglomerations with a larger size than the other variations.

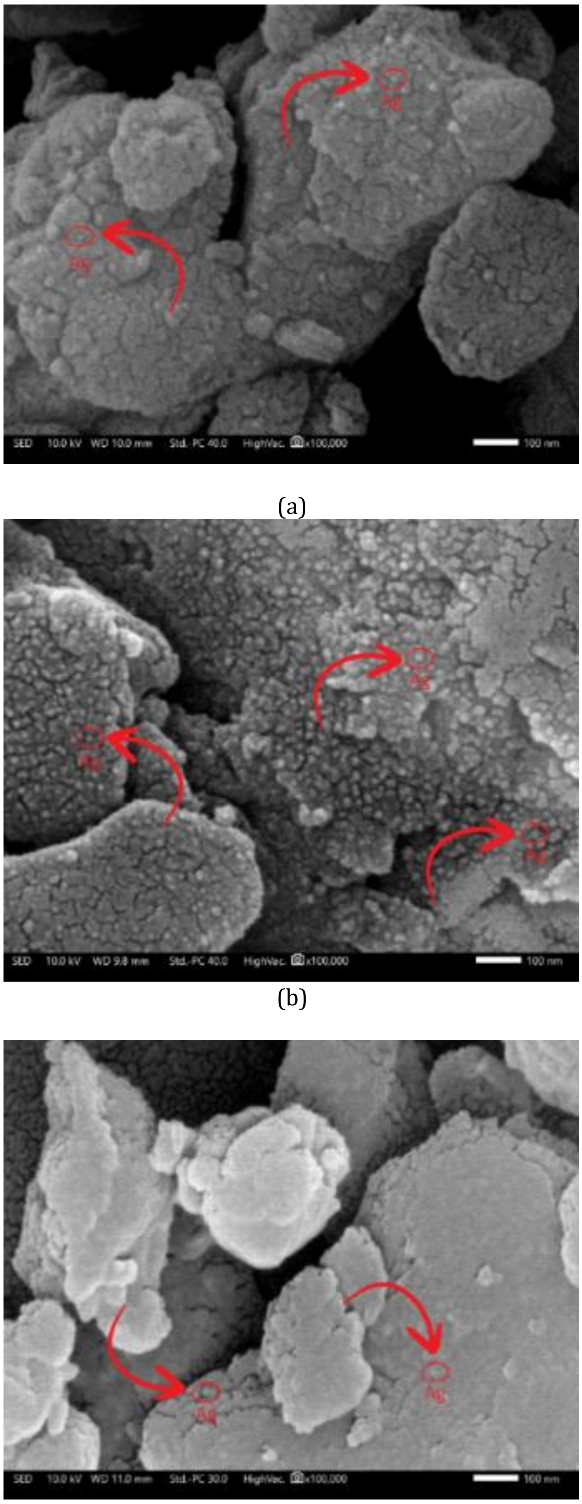

(a)

(b)

(c)

Fig. 2: FESEM images of AgNPs (a) A1, (b) A2, and (c) A3

Then, EDX characterization is used to determine the chemical composition of nanoparticles. The EDX spectrum graph in Fig. 3 shows an optical absorption peak in the 2.5-3.5 keV range, which indicates the presence of silver nanoparticles [30]. Based on the graph in Fig. 3, AgNPs with black betel leaf extract contain three elements, namely Ag (Silver), C (carbon), and O (Oxygen). Silver (Ag) was the dominant element, with mass percentages of 96.17%, 78.80%, and 49.14% in samples A1, A2, and A3, respectively. This indicates that the AgNPs synthesis in this study was quite effective, but not perfect. The elemental composition of AgNPs is shown in Table 2.

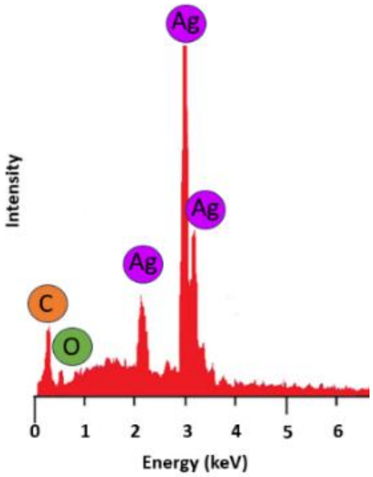

(a)

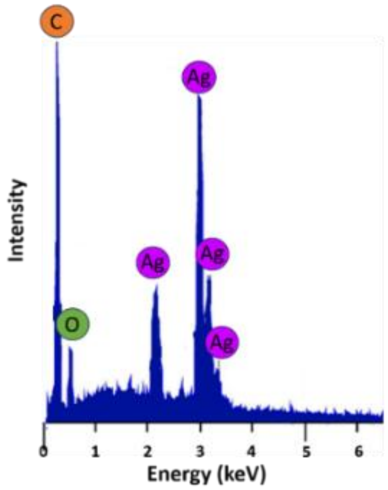

(b)

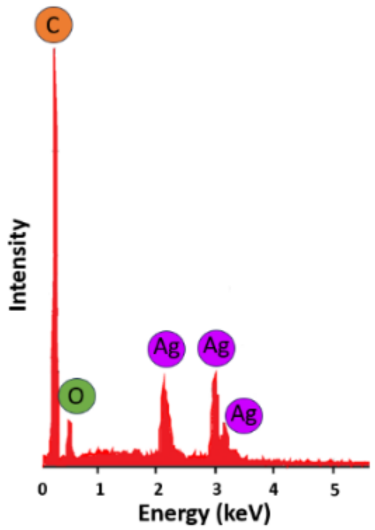

(c)

Fig. 3: EDX spectrum of AgNPs (a) A1, (b) A2, and (c) A3

Table 2: Mass Percentages og AgNPs

Element	Mass Percentages (%)		
	A1	A2	A3
Ag	96.17	78.80	49.14
O	1.37	5.44	8.20
C	2.46	15.76	42.66

The presence of carbon (C) and oxygen (O) in the samples confirms the organic content from the black betel leaf extract. Additionally, the C and O content is also attributed to incompletely reduced compounds from citric acid and PVA. Based on Table 2, variation A1 has the highest silver (Ag) elemental composition, making it the most promising as an antibacterial agent.

3.3. X-ray diffraction (XRD) analysis

X-Ray Diffraction (XRD) is a material characterization technique used to determine the structure and crystallinity data of AgNPs[20]. XRD testing utilizes an X-ray source with a Cu anode material that has a wavelength of 1.5406 Å. The XRD diffraction pattern produces peaks that are qualitatively analyzed to identify the material.

Fig. 3 shows the diffraction angles of AgNPs at five peaks—38.1°, 44.2°, 64.4°, 77.4°, and 81.5°—correspond to the formed phase. These peaks align with ICSD data no: 01-087-0597, representing characteristic peaks with Miller indices of (111), (200), (220), (311), and (222). The observed Miller indices are associated with Bragg reflections, which are consistent with the Face Centered Cubic (FCC) crystal lattice planes [20], [31].

The crystallite size of the silver nanoparticles was calculated using the Debye-Scherrer equation. The crystallite sizes for variations A1, A2, and A3 were 10.9 nm, 11.7 nm, and 11.3 nm, respectively. Based on this data, the crystallite size is smaller than the particle size observed in the FESEM analysis [32]. The XRD analysis indicates that AgNPs variation A1 has the smallest crystallite size, while the 1-gram grammage variation has the largest.

3.4. FTIR spectrophotometer analysis

The functional groups of the AgNPs and black betel leaf extract were determined using an FTIR spectrophotometer. The 3449 cm^{-1} band in the black curve is identical to the 3428 cm^{-1} band in the red curve. This indicates the presence of O-H stretching linked to hydrogen in the carboxylic acids found in the black betel leaf extract. It also underscores black betel leaf's role as a reducing agent for silver nanoparticles (Rashid et al., 2016). The red curve shows a weak peak at 2927 cm^{-1}, signifying C-H alkane bonds. Both the 2085 cm^{-1} band in the black curve and the 2224 cm^{-1} band in the red curve point to C=C bonds.

Specifically, the black curve suggests C=C alkene bonds, while the red curve indicates C=C aromatic bonds [33]. Peaks at 1636 cm^{-1} and 1599 cm^{-1} are attributable to C=O bonds, confirming the presence of carbonyl (aldehyde) groups. Additionally, C-O bonds are visible in both curves at 1079 cm^{-1}. The changes in these functional groups after AgNP formation indicate that biomolecules from black betel leaf extract interacted with AgNPs and acted as reducing and stabilizing agents during silver nanoparticle synthesis [34].

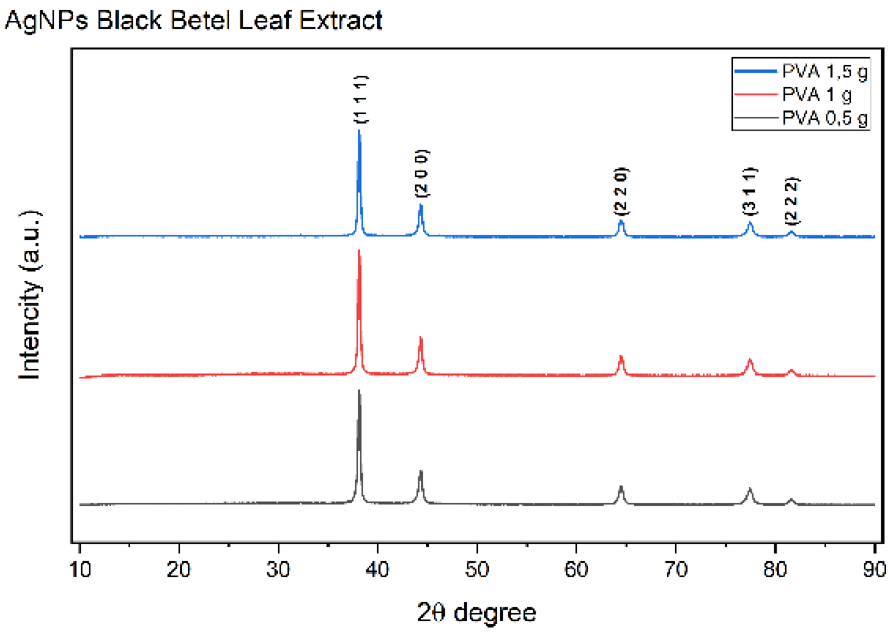

Fig. 4: XRD pattern of AgNPs

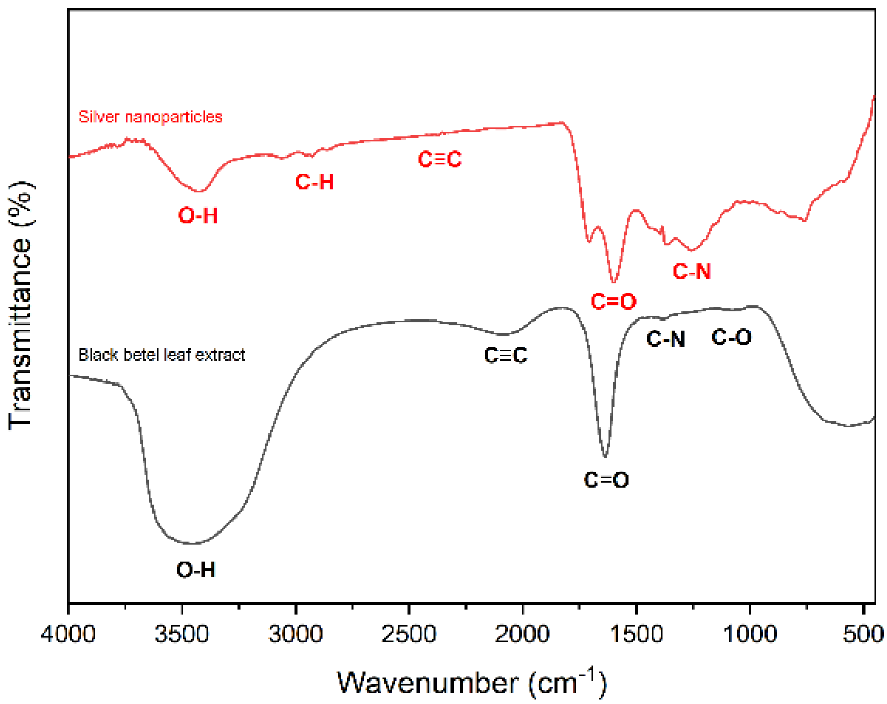

Fig. 5: FTIR pattern of AgNPs

The FTIR spectrum of the AgNPs are surrounded by various organic molecules, including terpenoids, alcohols, ketones, aldehydes, and carboxylic acids. Research by [35] suggests that AgNPs associated with such organic molecules possess antibacterial potential.

3.5. Antibacterial Study

Antibacterial testing aims to determine the antibacterial activity of silver nanoparticles (AgNPs). The AgNPs tested were AgNPs biosynthesized with black betel leaf extract and 0.5-gram PVA. The testing employed the disk diffusion method on both Gram-positive bacteria (*Staphylococcus aureus*) and Gram-negative bacteria (*Escherichia coli*). The testing process is based on CLSI (Clinical and Laboratory Standards Institute) 2020 standards. The results of the antibacterial testing are shown in Fig. 6.

According to Fig. 6, AgNPs exhibited an inhibition zone of 13.9 mm against *E. coli* and 11.3 mm against *S. aureus*. This data clearly indicates that AgNPs possesses a greater inhibitory effect on *E. coli*. The structural differences between Gram-positive and Gram-negative bacterial cell walls significantly influence AgNPs' inhibitory power. Gram-negative bacteria have a thinner peptidoglycan layer, making them more susceptible to disruption by AgNPs. While the outer membrane of Gram-negative bacteria serves as protection, it is permeable to small, positively charged particles like AgNPs. This characteristic allows for greater interaction with the bacterial surface and subsequent entry into the cell. Conversely, Gram-positive bacteria lack an outer membrane but possess a thick peptidoglycan layer that is more difficult for AgNPs to penetrate [36].

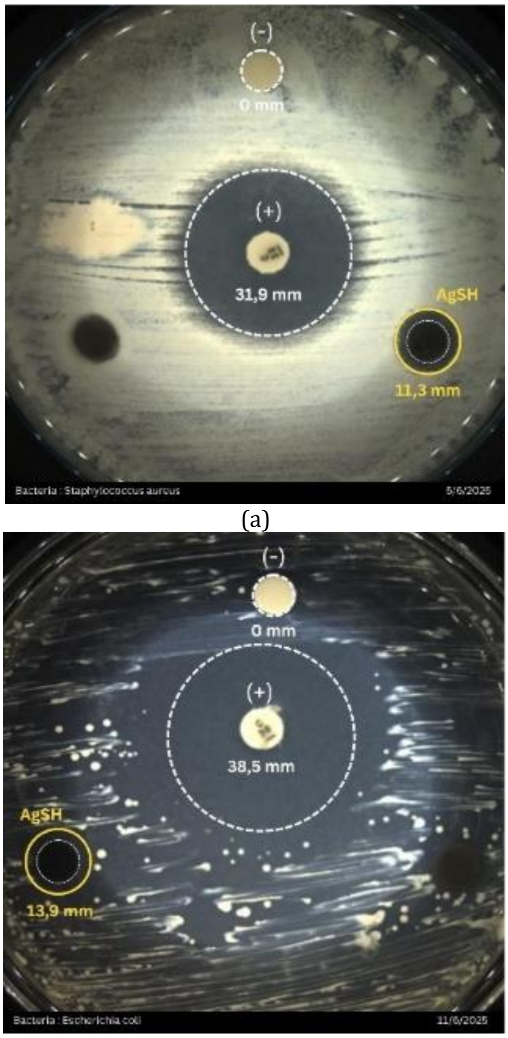

(a)

(b)

Fig. 6: Antibacterial activity of AgNPs (a) *S. aureus* and (b) *E. coli*

4. Conclusions

Silver nanoparticles (AgNPs) were successfully synthesized using a combination of black betel leaf extract and Polyvinyl alcohol (PVA). The AgNPs produced showed stable morphological characteristics, size, and elemental content, and had strong antibacterial activity against Escherichia coli and Staphylococcus aureus. This study successfully proved the effectiveness of black betel leaf extract as a bioreductor in the synthesis of AgNPs and presented an alternative method that is more environmentally friendly.

Acknowledgment

This work received financial support from Universitas Sebelas Maret under the Fundamental Research Grant with contract number 462/UN27.22/PT.01.03/2026.

References

[1] A. Ramani, S. Taherabbas, R. Saji, M. Bumbadiya, K. Gandhi, and R. Seth, “Nanotechnology: An emerging trend in the dairy industry – Applications and future challenges,” *Food Humanit.*, vol. 3, no. June, p. 100409, 2024, doi: 10.1016/j.foohum.2024.100409.

[2] F. A. Fabiani, F. Sutanti, D. Silvia, and M. A. Putri, “Green Synthesis Nanopartikel Perak Menggunakan Ekstrak Daun Pucuk Idat (Cratoxylum glaucum) sebagai Bioreduktor,” *Indones. J. Pure Appl. Chem.*, no. December 2018, 2019, doi: 10.26418/indonesian.v1i2.30533.

[3] T. A. Saleh, “Nanomaterials: Classification, properties, and environmental toxicities,” *Environ. Technol. Innov.*, vol. 20, p. 101067, 2020, doi: 10.1016/j.eti.2020.101067.

[4] S. Khan, S. Singh, S. Gaikwad, N. Nawani, M. Junnarkar, and S. V. Pawar, “Optimization of process parameters for the synthesis of silver nanoparticles from Piper betle leaf aqueous extract, and evaluation of their antiphytofungal activity,” *Environ. Sci. Pollut. Res.*, vol. 27, no. 22, pp. 27221–27233, 2020, doi: 10.1007/s11356-019-05239-2.

[5] K. M. Aboelghait, W. E. Abdallah, I. Abdelfattah, and A. M. El-Shamy, “Green synthesis of silver nanoparticles by waste of Murcott Mandarin peel as a sustainable approach for efficient heavy metal removal from metal industrial wastewater,” *Sep. Purif. Technol.*, vol. 347, no. February, p. 127609, 2024, doi: 10.1016/j.seppur.2024.127609.

[6] M. Ghasemi, M. Govahi, and H. R. Litkohi, “Green synthesis of silver nanoparticles (AgNPs) and chitosan-coated silver nanoparticles (CS-AgNPs) using Ferula gummosa Boiss. gum extract: A green nano drug for potential applications in medicine,” *Int. J. Biol. Macromol.*, vol. 291, no. September 2024, p. 138619, 2025, doi: 10.1016/j.ijbiomac.2024.138619.

[7] C. Nirmala, H. K. Bajwa, and S. Oinam, “Advances in Bamboo Science Bamboo mediated green synthesis of silver nanoparticles-A new approach towards utilization of an underutilized plant,” *Adv. Bamboo Sci.*, vol. 6, no. February, p. 100061, 2024, doi: 10.1016/j.bamboo.2024.100061.

[8] K. Karuppiah, K. Rajendran, B. Manickam Dakshinamoorthi, A. A. P. Thomas, and V. Rajaraman, "Structural characterization, spectral investigation and antimicrobial studies Of ZnWO4 and Zn0.9Cu0.1WO4 nanoparticles synthesized by microwave and sucrose mediated solgel method," *J. Mol. Struct.*, vol. 1253, p. 132067, 2022, doi: 10.1016/j.molstruc.2021.132067.

[9] B. Tessema, G. Gonfa, and S. Mekuria, "Synthesis and evaluation of the anti-bacterial effect of modified silica gel supported silver nanoparticles on E . coli and S . aureus," *Results Chem.*, vol. 7, no. November 2023, p. 101471, 2024, doi: 10.1016/j.rechem.2024.101471.

[10] M. Namakka, M. R. Rahman, K. A. M. Bin Said, M. Abdul Mannan, and A. M. Patwary, "A review of nanoparticle synthesis methods, classifications, applications, and characterization," *Environ. Nanotechnology, Monit. Manag.*, vol. 20, no. September, p. 100900, 2023, doi: 10.1016/j.enmm.2023.100900.

[11] E. Mohammadi and S. M. Amini, "Green synthesis of stable and biocompatible silver nanoparticles with natural flavonoid apigenin," *Nano-Structures and Nano-Objects*, vol. 38, no. May, p. 101175, 2024, doi: 10.1016/j.nanoso.2024.101175.

[12] D. Bokov *et al.*, "Nanomaterial by Sol-Gel Method: Synthesis and Application," *Adv. Mater. Sci. Eng.*, vol. 2021, 2021, doi: 10.1155/2021/5102014.

[13] J. Jalab, W. Abdelwahed, A. Kitaz, and R. Al-Kayali, "Green synthesis of silver nanoparticles using aqueous extract of Acacia cyanophylla and its antibacterial activity," *Heliyon*, vol. 7, no. 9, p. e08033, 2021, doi: 10.1016/j.heliyon.2021.e08033.

[14] P. Taba, N. Y. Parmitha, and S. Kasim, "Synthesis of Silver Nanoparticles Using Syzygium polyanthum Extract as Bioreductor and the Application as Antioxidan," *J. Chem. Res*, vol. 7, no. 1, pp. 51–60, 2019.

[15] R. Maharani and A. Fernandes, "Profil fitokimia dan GC-MS daun sirih hitam (Piper betle L.) dari sekitar khdik Labanan, Kabupaten Berau," *Maj. Farm. dan Farmakol.*, vol. 25, no. 1, pp. 11–14, 2021, doi: 10.20956/mff.v25i1.11966.

[16] V. T. Tran, T. B. Nguyen, H. C. Nguyen, N. H. N. Do, and P. K. Le, "Recent applications of natural bioactive compounds from Piper betle (L.) leaves in food preservation," *Food Control*, vol. 154, no. July, p. 110026, 2023, doi: 10.1016/j.foodcont.2023.110026.

[17] A. Ounkaew, N. Janaum, P. Kasemsiri, M. Okhawilai, S. Hiziroglu, and P. Chindaprasirt, "Synergistic effect of starch/polyvinyl alcohol/citric acid films decorated with in-situ green-synthesized nano silver on bioactive packaging films," *J. Environ. Chem. Eng.*, vol. 9, no. 6, p. 106793, 2021, doi: 10.1016/j.jece.2021.106793.

[18] D. Apriandanu, S. Wahyuni, S. Hadisaputro, and Harjono, "Sintesis Nanopartikel Perak Menggunakan Metode Poliol dengan Agen Stabilisator Polivinilalkohol (PVA)," *J. MIPA*, vol. 2, no. 36, pp. 157–168, 2013.

[19] M. Lu, S. Chadha, Saruchi, and V. Kumar, "Fabrication of silver nanoparticles synthesize using Lantana camara leaves extract on biofilm of sodium alginate," *J. Indian Chem. Soc.*, vol. 101, no. 8, p. 101189, 2024, doi: 10.1016/j.jics.2024.101189.

[20] M. Y. Nassar *et al.*, "Synthesis and characterization of lemon leaf extract-mediated silver nanoparticles: An environmentally friendly approach with enhanced antibacterial efficacy," *J. Mol. Struct.*, vol. 1315, no. May, p. 138753, 2024, doi: 10.1016/j.molstruc.2024.138753.

[21] N. T. Nguyen, T. H. Vu, and V. H. Bui, "Antibacterial and Antifungal Fabrication of Natural Lining Leather Using Bio-Synthesized Silver Nanoparticles from Piper Betle L. Leaf Extract," *Polymers (Basel).*, vol. 15, no. 12, 2023, doi: 10.3390/polym15122634.

[22] S. J. bakht Dalir, H. Djahaniani, F. Nabati, and M. Hekmati, "Characterization and the evaluation of antimicrobial activities of silver nanoparticles biosynthesized from Carya illinoinensis leaf extract," *Heliyon*, vol. 6, no. 3, p. e03624, 2020, doi: 10.1016/j.heliyon.2020.e03624.

[23] A. Lagashetty, S. K. Ganiger, and Shashidhar, "Synthesis, characterization and antibacterial study of Ag–Au Bi-metallic nanocomposite by bioreduction using piper betle leaf extract," *Heliyon*, vol. 5, no. 12, p. e02794, 2019, doi: 10.1016/j.heliyon.2019.e02794.

[24] I. N. Oktavia and S. Sutoyo, "Review Artikel: Sintesis Nanopartikel Perak Menggunakan Bioreduktor Ekstrak Tumbuhan Sebagai Bahan Antioksidan," *Unesa J. Chem.*, vol. 10, no. 1, pp. 37–54, 2021, doi: 10.26740/ujc.v10n1.p37-54.

[25] V. Veena, K. . Shivaprasad, H. Sharanaguoda, G. K. Sangappa, and A. Lagashetty, "Facile synthesis, characterization, insilico modelling, and bioinformatic study of dimercapto-triazole functionalized silver nanoparticles," *Results Chem.*, vol. 7, no. December 2023, p. 101351, 2024, doi: 10.1016/j.rechem.2024.101351.

[26] J. Car and N. Krstulovi, "Analytical Model for Determination of Size-Distribution of Colloidal Silver Nanoparticles from Surface Plasmon Resonance Wavelength and Dielectric Functions," *Nanomaterials*, vol. 12, no. 19, p. 3474, 2022, doi:

10.3390/nano12193474.
[27] M. Shahjahan, "Synthesis and Characterization of Silver Nanoparticles by Sol-Gel Technique," *Nanosci. Nanometrology*, vol. 3, no. 1, p. 34, 2017, doi: 10.11648/j.nsnm.20170301.16.
[28] A. N. Nalawati, N. E. Suyatma, and D. I. Wardhana, "Sintesis Nanopartikel Perak (NPAg) dengan Bioreduktor Ekstrak Biji Jarak Pagar dan Kajian Aktivitas Antibakterinya," *J. Teknol. dan Ind. Pangan*, vol. 32, no. 1, pp. 98–106, 2021, doi: 10.6066/jtip.2021.32.2.98.
[29] T. Prasetyaningtyas, A. T. Prasetya, and N. Widiarti, "Sintesis Nanopartikel Perak Termodifikasi Kitosan dengan Bioreduktor Ekstrak Daun Kemangi (Ocimum Basilicum L.) dan Uji Aktivitasnya sebagai Antibakteri," *Indones. J. Chem. Sci.*, vol. 9, no. 1, pp. 37–43, 2020, [Online]. Available: https://journal.unnes.ac.id/sju/index.php/ijcs/article/view/29927/15739
[30] K. O. Saygi and E. Cacan, "Antioxidant and cytotoxic activities of silver nanoparticles synthesized using Tilia cordata flowers extract," *Mater. Today Commun.*, vol. 27, no. December 2020, p. 102316, 2021, doi: 10.1016/j.mtcomm.2021.102316.
[31] S. Kazemi *et al.*, "Recent advances in green synthesized nanoparticles: from production to application," *Mater. Today Sustain.*, vol. 24, p. 100500, 2023, doi: 10.1016/j.mtsust.2023.100500.
[32] S. Nasiri *et al.*, "Modified Scherrer equation to calculate crystal size by XRD with high accuracy, examples Fe2O3, TiO2 and V2O5," *Nano Trends*, vol. 3, no. August, p. 100015, 2023, doi: 10.1016/j.nwnano.2023.100015.
[33] D. D. Joshi, "Herbal Drugs and Fingerprints," *Herb. Drugs Fingerprints*, pp. 121–146, 2012, doi: 10.1007/978-81-322-0804-4.
[34] S. Pasieczna-patkowska and M. Cichy, "Application of Fourier Transform Infrared (FTIR) Spectroscopy in Characterization of Green Synthesized Nanoparticles," *Molecules*, vol. 30, no. 3, p. 684, 2025, doi: 10.3390/molecules30030684.
[35] S. Praba, J. Jeyasundari, Y. Brightson, and A. Jacob, "Synthesis of Silver Nano Particles Using Piper Betle and Its Antibacterial Activity," *Chem. Bull*, vol. 3, no. 10, pp. 1014–1016, 2014.
[36] S. S. Behera *et al.*, "Green synthesis of silver-chitosan nanocomposite exhibits promising antibiofilm properties against pathogenic bacteria Escherichia coli and Staphylococcus aureus," *Microbe (Netherlands)*, vol. 6, no. October 2024, p. 100264, 2025, doi: 10.1016/j.microb.2025.100264.